
Effective End-to-end Unsupervised Outlier Detection via Inlier Priority of Discriminative Network

Siqi Wang^{1*}, Yijie Zeng^{2*}, Xinwang Liu¹, En Zhu¹, Jianping Yin³, Chuanfu Xu¹, Marius Kloft⁴

¹National University of Defense Technology, ²Nanyang Technological University

³Dongguan University of Technology, ⁴Technische Universität Kaiserslautern

wangsiqi10c@nudt.edu.cn, yzeng004@e.ntu.edu.sg, {xinwangliu, enzhu}@nudt.edu.cn

jpyin@dgut.edu.cn, xuchuanfu@nudt.edu.cn, kloft@cs.uni-kl.de

Abstract

Despite the wide success of deep neural networks (DNN), little progress has been made on end-to-end unsupervised outlier detection (UOD) from high dimensional data like raw images. In this paper, we propose a framework named *E³Outlier*, which can perform UOD in a both *effective* and *end-to-end* manner: First, instead of the commonly-used autoencoders in previous end-to-end UOD methods, *E³Outlier* for the first time leverages a discriminative DNN for better representation learning, by using *surrogate supervision* to create multiple pseudo classes from original unlabelled data. Next, unlike classic UOD that utilizes data characteristics like density or proximity, we exploit a novel property named *inlier priority* to enable end-to-end UOD by discriminative DNN. We demonstrate theoretically and empirically that the intrinsic class imbalance of inliers/outliers will make the network prioritize minimizing inliers' loss when inliers/outliers are indiscriminately fed into the network for training, which enables us to differentiate outliers directly from DNN's outputs. Finally, based on inlier priority, we propose the negative entropy based score as a simple and effective outlierness measure. Extensive evaluations show that *E³Outlier* significantly advances UOD performance by up to 30% AUROC against state-of-the-art counterparts, especially on relatively difficult benchmarks.

1 Introduction

An outlier is defined as “an observation which deviates so much from the other observations as to arouse suspicions that it was generated by a different mechanism” [1]. In some context of the literature, outliers are also referred as anomalies, deviants, novelties or exceptions [2]. Outlier detection (OD) has broad applications such as financial fraud detection [3], intrusion detection [4], fault detection [5], etc. Various solutions have been proposed to tackle OD (see [6] for a comprehensive review). Based on the availability of labels, those solutions can be accordingly divided into three categories below [7]: **1) Supervised** OD (SOD) deals with the case where a training set is provided with both labelled inliers/outliers, but it suffers from expensive data labelling and the rarity of outliers in practice [6]. **2) Semi-supervised** OD (SSOD) only requires pure single-class training data that are labelled as “inlier” or “normal”, and no outlier is involved during training. **3) Unsupervised** OD (UOD) handles completely unlabelled data mixed with outliers, and no data label is provided for training at all.

In this paper we will limit our discussion to **UOD**, as most data are unlabelled in practice and UOD is the most widely applicable [7]. In particular, two *clarifications of concepts* must be made: First, in some literature like [8, 9], “unsupervised outlier/anomaly detection” actually refers to SSOD rather than UOD by our definition. Second, a recent topic is *out-of-distribution sample detection*, which

* Authors contribute equally.

detects samples that are not from the distribution of training samples [10, 11, 12]. It is similar to SSOD, but it requires well-labelled multi-class data for training rather than single-class data in SSOD. Both cases above are different from UOD that does not use any label information in this paper.

Recently, surging image/video data have inspired important UOD applications in computer vision, e.g. refining web image query results [13] and video abnormal event detection [14]. Unfortunately, despite the remarkable success of end-to-end deep neural networks (DNN) in computer vision [15], an *effective* and *end-to-end* UOD strategy is still under exploration: State-of-the-art methods [16, 17, 18] unexceptionally rely on deep autoencoders (AE) or convolutional autoencoders (CAE) to realize easily achievable DNN based UOD, but they all suffer from AE/CAE’s ineffective representation learning (detailed in Sec. 3.1). Motivated by this gap, we aim to address UOD in a both effective and end-to-end fashion, with the application to detect outlier images from contaminated datasets.

Contributions. This paper proposes an *effective* and *end-to-end* UOD framework named E^3 *Outlier*. Specifically, our contributions can be summarized below: **1)** To liberate DNN based UOD from AE/CAE’s ineffective representation learning, E^3 *Outlier* for the first time enables us to adopt powerful discriminative DNN architectures like ResNet [19] for representation learning in UOD. This is realized by *surrogate supervision*, which creates multiple pseudo classes by imposing various simple operations on original unlabelled data. **2)** E^3 *Outlier* discovers outliers based on a novel property of discriminative network named *inlier priority*, which evidently differs from previous methods that utilize certain data characteristics (e.g. density, proximity, distance) to perform UOD. Through both theory and experiments, we demonstrate that inlier priority will encourage the network to prioritize the reduction of inliers’ loss during network training. On the foundation of inlier priority, E^3 *Outlier* is able to achieve end-to-end UOD by directly inspecting the DNN’s outputs, which reflect each datum’s priority level. In this way, it avoids the possible suboptimal performance yielded by feeding the DNN’s learned representations into a decoupled UOD method [20]. **3)** Based on inlier priority, we explore several strategies and propose a simple and effective negative entropy based score to measure outlierness. Extensive experiments report a remarkable improvement by E^3 *Outlier* against state-of-the-art methods, particularly on relatively difficult benchmarks for unsupervised tasks.

2 Related Work

Classic Outlier Detection. For classic SOD, labelled data are utilized to build discriminative models by well-studied supervised binary/multi-class classification techniques, such as support vector machine (SVM) [21], random forest [22] and recent XGBoost [23]. In contrast, SSOD that requires only labelled inliers is much more prevalent, and it is also called *one-class classification* [24] or *novelty detection* [25]. Classic SSOD usually involves training a model on pure inliers and detecting those data that evidently deviate from this model as outliers, and representative SSOD methods include SVM based methods [26, 27], replicator network/autoencoders [28, 29], principle component analysis (PCA)/kernel based PCA [30, 31]. Compared with SOD and SSOD, UOD handles the most challenging case where no labelled data is available. Classic UOD methods discover outliers by examining the basic characteristics of data, such as statistical properties [32], cluster membership [33, 34], density [35, 36, 37], proximity [38, 39], etc. Besides, ensemble methods like isolation forest [40] and its variants [41, 42] are popular in UOD. However, most state-of-the-art UOD methods like [40, 37, 13] still require manual feature extraction from high dimensional data like raw images.

DNN based Outlier Detection. DNN’s recent success naturally inspires DNN based OD [20]. For SOD, discriminative DNN can be directly applied, while the main issue is the class imbalance of inliers/outliers [20], which is explored by [43, 44, 45, 46]. For SSOD, the case is more difficult as only labelled inliers are provided. DNN solutions for SSOD fall into three types: Mainstream DNN based SSOD methods handle high dimensional data by label-free generative models, i.e. AE/CAE [47, 48, 49, 50] and generative adversarial network (GAN) [51, 52, 53]. The second type extends classic SSOD methods into their deep counterparts, such as deep support vector data description [54] and deep one-class SVM [55]. The last type turns SSOD into SOD by certain means like introducing reference datasets [56], intra-class splitting [57], geometric transformations [58] or synthetic outlier generation [59]. As to UOD, the absence of both inlier and outlier label poses great challenges to combining UOD with DNN, which results in much less progress than SOD and SSOD. In addition to the naive solution that feeds DNN’s learned representations into a separated UOD method [20], to our best knowledge only the following works have explored DNN based UOD: Zhou et al. [17] propose a decoupled solution that combines a deep AE with Robust PCA, which decomposes the inputs into a

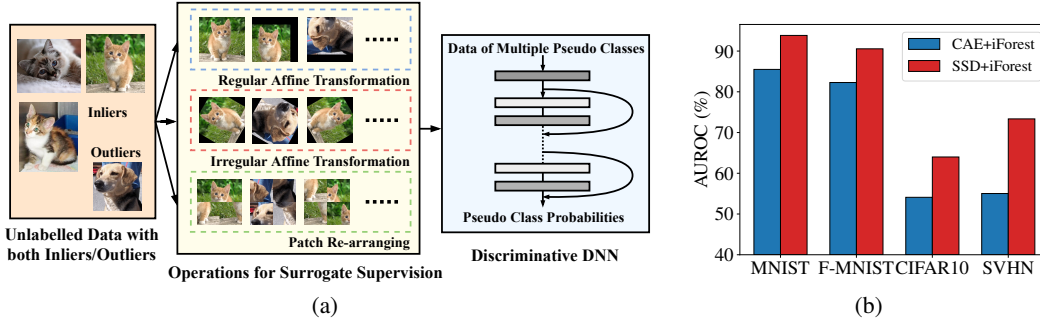


Figure 1: Surrogate supervision workflow (left) and the comparison of learned representations (right).

low-rank part from inliers and a sparse part from outliers; For end-to-end UOD, Xia et al. [16] use deep AE directly and propose a variant that estimates inliers by seeking a threshold that maximizes the inter-class variance of AE’s reconstruction loss. A loss function is designed to encourage the separation of estimated inliers/outliers; Zong et al. [18] jointly optimize a deep AE and an estimation network to perform simultaneous representation learning and density estimation for end-to-end UOD.

Surrogate Supervision. Recent studies propose surrogate supervision to improve DNN pre-training for downstream high-level tasks like image classification and object detection. It imposes certain operations on unlabelled data to create corresponding pseudo classes and provide supervision signal, such as rotation [60], image patch permutation [61], clustering [62], etc. Surrogate supervision is also called self-supervision (see [63] for a comprehensive survey), but we use surrogate supervision to better distinguish it from AE/CAE, which are also viewed as “self-supervised” in some context. To our best knowledge, our work is the first to connect surrogate supervision with end-to-end UOD.

3 The proposed E^3 Outlier Framework

Problem Formulation of UOD. Considering a data space \mathcal{X} (in this context the space of images), an unlabelled data collection $X \subseteq \mathcal{X}$ consists of an inlier set X_{in} and an outlier set X_{out} , which originate from fundamentally different underlying distributions [1]. Our goal is to obtain an end-to-end UOD method $S(\cdot)$ that in the ideal case outputs $S(\mathbf{x}) = 1$ for inlier $\mathbf{x} \in X_{in}$ and $S(\mathbf{x}) = 0$ for outlier $\mathbf{x} \in X_{out}$. In practice, a smaller $S(\mathbf{x})$ indicates a higher likelihood of \mathbf{x} to be an outlier.

3.1 Surrogate Supervision Based Effective Representation Learning for UOD

Why NOT AE/CAE? We note that existing DNN based UOD methods rely on AE/CAE [16, 17, 18]. However, it is hard for them to handle relatively complex datasets like CIFAR10 and SVHN: As our UOD experiments² show in Fig. 1(b), even a sophisticated deep CAE with isolation forest [40] only performs slightly better than random guessing (50% AUROC). Similar results are reported in other AE/CAE based unsupervised tasks like deep clustering [64, 65]. This is because AE/CAE typically adopt mean square error (MSE) as loss function, which forces AE/CAE to focus on reducing low-level pixel-wise error that is not sensitive to human perception, rather than learning high-level semantic features [66, 67]. Therefore, AE/CAE based representation learning is often ineffective.

Surrogate Supervision. Discriminative DNNs like ResNet [19] and Wide ResNet (WRN) [68] have proved to be highly effective in learning high-level semantic features, but they have not been explored in UOD due to the lack of supervision. To remedy the absence of data labels and substitute AE/CAE, we propose a *surrogate supervision based discriminative network* (SSD) for more effective representation learning in UOD. Specifically, we first define an operation set with K operations $\mathcal{O} = \{O(\cdot|y)\}_{y=1}^K$, where y represents the pseudo label associated with the operation $O(\cdot|y)$. Applying an operation $O(\cdot|y)$ to \mathbf{x} can generate a new datum $\mathbf{x}^{(y)} = O(\mathbf{x}|y)$, and all data generated by the operation $O(\cdot|y)$ belong to the pseudo class with pseudo label y . Next, given a datum $\mathbf{x}^{(y')}$, a discriminative DNN with a K -node softmax layer is trained to classify the type of applied

²All UOD experiments in Sec. 3 follow the setup detailed in Sec. 4.1 and the outlier ratio is fixed to 10%.

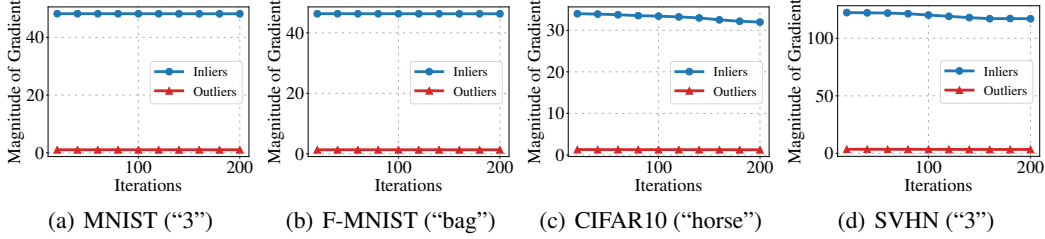


Figure 2: Inliers and outliers’ gradient magnitude on example cases of benchmark datasets during SSD training. The class used as inliers is in brackets.

operation, i.e. the DNN is supposed to classify $\mathbf{x}^{(y')}$ into the y' -th pseudo class. With $P^{(y)}(\cdot)$ and θ denoting the probability output by the y -th node of softmax layer and DNN’s learnable parameters respectively, DNN’s output probability vector for K operations is $P(\mathbf{x}^{(y')}|\theta) = [P^{(y)}(\mathbf{x}^{(y')}|\theta)]_{y=1}^K$. To train such a DNN with an unlabelled data collection $X = \{\mathbf{x}_i\}_{i=1}^N$, the objective function is:

$$\min_{\theta} \frac{1}{N} \sum_{i=1}^N \mathcal{L}_{SS}(\mathbf{x}_i|\theta) \quad (1)$$

where $\mathcal{L}_{SS}(\mathbf{x}_i|\theta)$ is the loss incurred by \mathbf{x}_i under surrogate supervision. When the commonly-used cross entropy loss is used to classify pseudo classes of surrogate supervision, it can be written as:

$$\mathcal{L}_{SS}(\mathbf{x}_i|\theta) = -\frac{1}{K} \sum_{y=1}^K \log(P^{(y)}(\mathbf{x}_i^{(y)}|\theta)) = -\frac{1}{K} \sum_{y=1}^K \log(P^{(y)}(O(\mathbf{x}_i|y)|\theta)). \quad (2)$$

As to the operation set \mathcal{O} , each operation $O(\cdot|y) \in \mathcal{O}$ is defined as a combination of one or more basic transformations from the following transformation sets: **1) Rotation**: This set’s transformations clock-wisely rotate images by a certain degree. **2) Flip**: This set’s transformations refer to flipping the image or not. **3) Shifting**: This set’s transformations shift the image by some pixels along x -axis or y -axis. **4) Patch re-arranging**: This set’s transformations partition the image into several equally-sized patches and re-organize them into a new image by a certain permutation. Based on them, we construct three operation subsets, i.e. regular affine transformation set \mathcal{O}_{RA} , irregular affine transformation set \mathcal{O}_{IA} and patch re-arranging set \mathcal{O}_{PR} (detailed in Sec.1 in supplementary material). The final operation set is $\mathcal{O} = \mathcal{O}_{RA} \cup \mathcal{O}_{IA} \cup \mathcal{O}_{PR}$, and Fig. 1(a) shows SSD’s entire workflow. To verify SSD’s effectiveness, we extract the outputs of its penultimate layer as the learned representations, while the outputs of deep CAE’s intermediate hidden layer (with the same dimension as SSD) are used for comparison. We feed them into isolation forest [40], which is generally acknowledged to be a good UOD method [69], to perform UOD under the same parameterization. As shown in Fig. 1(b), SSD’s learned representations are able to outperform CAE by a large margin (8%-10% AUROC).

3.2 Inlier Priority: The Foundation of End-to-end UOD

Motivation. The above simple solution feeds SSD’s learned representations into a decoupled UOD method, which may yield suboptimal performance because SSD and the UOD method are trained separately [18, 20]. Our goal is to achieve end-to-end UOD without using a decoupled UOD method. Recall that outliers are essentially rare patterns in a data collection [7], which implies an intrinsic *class imbalance* between inliers/outliers. Class imbalance is unfavorable in machine learning as it leads to the bias towards majority class during training [70, 71]. However, we argue that class imbalance can be favorably exploited in UOD as it gives rise to “*inlier priority*”: ***Despite that inliers/outliers are indiscriminately fed into SSD for training, SSD will prioritize the minimization of inliers’ loss.*** This intuition naturally inspires an end-to-end UOD solution by measuring how well the SSD’s output of a datum matches its target pseudo label, which directly indicates its priority level in training and the likelihood to be an inlier. We demonstrate the inlier priority in terms of two aspects below:

Priority by Gradient Magnitude. *Our first point is that inliers will produce gradient with stronger magnitude to update the SSD network than outliers.* To demonstrate this point, we consider an SSD

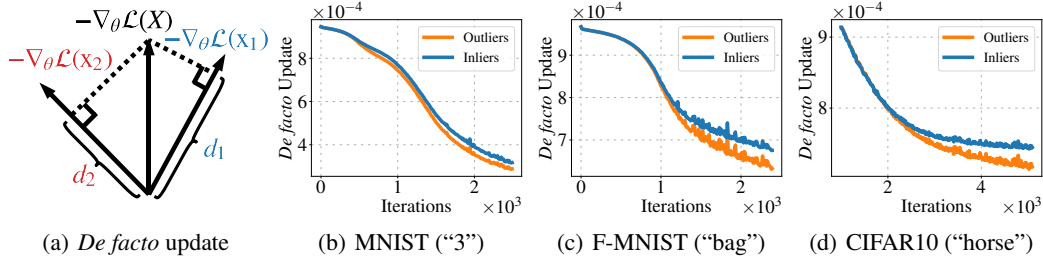


Figure 3: An illustration of *de facto* update and some example cases of the average *de facto* update for inliers/outliers during the network training. The class used as inliers is in brackets.

with its network weights randomly initialized by i.i.d. uniform distribution on $[-1, 1]$. Without loss of generality, we consider the gradients w.r.t. the weights associated with the c -th class ($1 \leq c \leq K$) between the penultimate layer and softmax layer, $\mathbf{w}_c = [w_{s,c}]_{s=1}^{(L+1)}$ ($w_{L+1,c}$ is bias), because these weights are directly responsible for making predictions. For the commonly-used cross-entropy loss \mathcal{L} , only data transformed by the c -th operation $X^{(c)} = \{O(\mathbf{x}|c) | \mathbf{x} \in X\}$ are used to update \mathbf{w}_c . The gradient vector incurred by \mathcal{L} is denoted by $\nabla_{\mathbf{w}_c}\mathcal{L} = [\nabla_{w_{s,c}}\mathcal{L}]_{s=1}^{(L+1)}$, which will be used to update \mathbf{w}_c in back-propagation based optimizer like Stochastic Gradient Descent (SGD) [72]. Given unlabelled data with N_{in} inliers and N_{out} outliers, it is easy to know that $X^{(c)}$ also contains N_{in} transformed inliers and N_{out} transformed outliers. Here we are interested in the magnitude of transformed inliers and outliers' aggregated gradient to update \mathbf{w}_c , i.e. $\|\nabla_{\mathbf{w}_c}^{(in)}\mathcal{L}\|$ and $\|\nabla_{\mathbf{w}_c}^{(out)}\mathcal{L}\|$, which directly reflect inliers/outliers' strength to affect the training of SSD. Since SSD is randomly initialized, we need to compute the expectation of gradient magnitude. As shown in Sec. 2 of supplementary material, for a simplified SSD network with a single hidden-layer and sigmoid activation, we can quantitatively derive the following approximation on inliers and outliers' gradient magnitude:

$$\frac{E(\|\nabla_{\mathbf{w}_c}^{(in)}\mathcal{L}\|^2)}{E(\|\nabla_{\mathbf{w}_c}^{(out)}\mathcal{L}\|^2)} \approx \frac{N_{in}^2}{N_{out}^2} \quad (3)$$

where $E(\cdot)$ denotes the probability expectation. As the class imbalance between inliers and outliers leads to $N_{in} \gg N_{out}$, we naturally yield $E(\|\nabla_{\mathbf{w}_c}^{(in)}\mathcal{L}\|) \gg E(\|\nabla_{\mathbf{w}_c}^{(out)}\mathcal{L}\|)$. Therefore, it serves as a theoretical indication that *the gradient magnitude induced by inliers will be significantly larger than outliers for an untrained SSD network*. Since it is particularly difficult to directly analyze more complex network architectures such as Wide ResNet [68], we empirically examine inliers and outliers' gradient magnitude during training by experiments (see Fig. 2), and the observations on different benchmarks are consistent with the above analysis on the simplified case: The magnitude of inliers' aggregated gradient has constantly been larger than outliers during the process of SSD training.

Priority by Network Updating Direction. *Our second point is that the network updating direction of SSD will bias towards the direction that prioritizes reducing inliers' loss during the SSD training.* Since training is dynamic and a theoretical analysis is intractable, we demonstrate this point using an empirical verification by computing inliers/outliers' average "*de facto* update": As illustrated by Fig. 3(a), consider a datum \mathbf{x}_i from a batch of data X , and its negative gradient $-\nabla_{\theta}\mathcal{L}(\mathbf{x}_i)$ is the fastest network updating direction to reduce \mathbf{x}_i 's loss. However, the network weights θ are actually updated by the negative gradient of the entire batch X , $-\nabla_{\theta}\mathcal{L}(X) = -\frac{1}{N}\sum_i \nabla_{\theta}\mathcal{L}(\mathbf{x}_i)$. It is actually different from the best updating direction for each individual datum. Thus, the *de facto* update d_i for \mathbf{x}_i refers to the actual gradient magnitude that \mathbf{x}_i obtains along its best direction for loss reduction from the network update direction $-\nabla_{\theta}\mathcal{L}(X)$, which can be computed by projecting $-\nabla_{\theta}\mathcal{L}(X)$ onto the direction of $-\nabla_{\theta}\mathcal{L}(\mathbf{x}_i)$: $d_i = -\nabla_{\theta}\mathcal{L}(X) \cdot \frac{-\nabla_{\theta}\mathcal{L}(\mathbf{x}_i)}{\|-\nabla_{\theta}\mathcal{L}(\mathbf{x}_i)\|}$. In this way, d_i reflects how much effort the network will devote to reduce \mathbf{x}_i 's loss, and it is a direct indicator of data's priority during network training. We calculate the average *de facto* update of inliers/outliers w.r.t the weights between SSD's penultimate and softmax layer and visualize some examples in Fig. 3(b)-3(d): Although the average *de facto* update of inliers/outliers is very close at the beginning, the average *de*

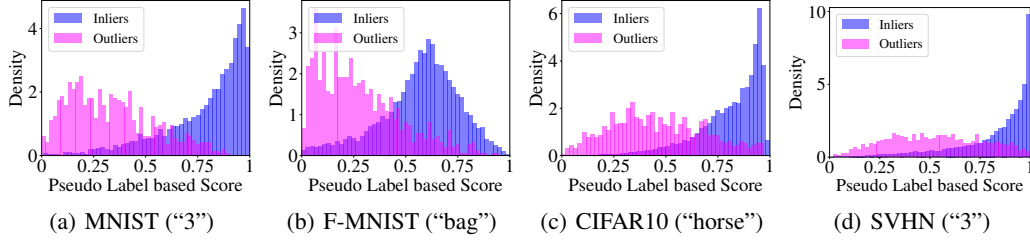


Figure 4: Normalized histograms of inliers/outliers’ $S_{pl}(\mathbf{x})$. The class used as inliers is in brackets.

facto update of inliers becomes evidently higher than outliers as the training continues, which implies that *SSD* will devote more efforts to reducing inliers’ loss by its network updating direction.

Remarks on Inlier Priority. 1) Based on the discussion above, inliers will gain priority in terms of both the gradient magnitude and the updating direction of *SSD*’s network weights. Such priority leads to a lower loss for inliers after training, which enables us to discern outliers by *SSD*’s outputs and serves as a foundation of end-to-end UOD. **2)** Intuitively, inlier priority will also happen when using AE/CAE based end-to-end UOD methods. However, the effect of inlier priority is severely diminished in this case for two reasons: First, AE/CAE typically uses the raw image pixels as learning targets, but the intra-class difference of inlier images can be very large, which means AE/CAE usually does not have a unified learning target like *SSD*. Second, AE/CAE is ineffective in learning high-level representations (as we discussed in Sec. 3.1), which makes it difficult to capture common high-level semantics of inlier images. Both factors above disable inliers from being a joint force to dominate the training of AE and produce a strong inlier priority effect like *SSD*, which is also demonstrated by AE/CAE’s poor UOD performance in empirical evaluation (see experimental results in Sec. 4.2).

3.3 Scoring Strategies for UOD

Based on inlier priority, we need a strategy $S(\cdot)$ to score a datum \mathbf{x} . Given $\mathbf{x}^{(y)} = O(\mathbf{x}|y)$ and the probability vector $P(\mathbf{x}^{(y)}|\boldsymbol{\theta})$ from *SSD*’s softmax layer, we explore three strategies below:

Pseudo Label based Score (PL): Inlier priority suggests that *SSD* will prioritize reducing inliers’ loss during training. For the datum $\mathbf{x}^{(y)}$, we note that the calculation of its cross entropy loss only depends on the probability $P^{(y)}(\mathbf{x}^{(y)}|\boldsymbol{\theta})$ that corresponds to its pseudo label y in $P(\mathbf{x}^{(y)}|\boldsymbol{\theta})$. Thus, we propose a direct scoring strategy $S_{pl}(\mathbf{x})$ by averaging $P^{(y)}(\mathbf{x}^{(y)}|\boldsymbol{\theta})$ for all K operations:

$$S_{pl}(\mathbf{x}) = \frac{1}{K} \sum_{y=1}^K P^{(y)}(\mathbf{x}^{(y)}|\boldsymbol{\theta}). \quad (4)$$

Maximum Probability based Score (MP): PL seems to be an ideal score. However, we note that operations for surrogate supervision do not always create sufficiently separable classes, e.g. image with a digit “8” is still an “8” when applying a flip operation. Hence, misclassifications will happen and the probability $P^{(y)}(\mathbf{x}^{(y)}|\boldsymbol{\theta})$ that corresponds to pseudo label y may not be the only or the best indicator to reflect how well the loss of a datum is reduced. Therefore, instead of $P^{(y)}(\mathbf{x}^{(y)}|\boldsymbol{\theta})$, we alternatively adopt the maximum probability of $P(\mathbf{x}^{(y)}|\boldsymbol{\theta})$ to calculate the score $S_{mp}(\mathbf{x})$ as follows:

$$S_{mp}(\mathbf{x}) = \frac{1}{K} \sum_{y=1}^K \max_t P^{(t)}(\mathbf{x}^{(y)}|\boldsymbol{\theta}). \quad (5)$$

Negative Entropy based Score (NE). Both strategies above rely on a single probability retrieved from $P(\mathbf{x}^{(y)}|\boldsymbol{\theta})$, while the information of the rest $(K - 1)$ classes’ probability is ignored. If we consider the entire probability distribution $P(\mathbf{x}^{(y)}|\boldsymbol{\theta})$, the training actually encourages *SSD* to output a probability distribution closer to the label’s one-hot distribution. With inlier priority, we can expect *SSD* to output a sharper probability distribution $P(\mathbf{x}^{(y)}|\boldsymbol{\theta})$ for inliers and a more uniform $P(\mathbf{x}^{(y)}|\boldsymbol{\theta})$

for outliers. Thus, we propose to use information entropy $H(\cdot)$ [73] as a simple and effective measure to the sharpness of a distribution, which gives the negative entropy based score $S_{ne}(\mathbf{x})$:

$$S_{ne}(\mathbf{x}) = -\frac{1}{K} \sum_{y=1}^K H(P(\mathbf{x}^{(y)}|\boldsymbol{\theta})) = \frac{1}{K} \sum_{y=1}^K \sum_{t=1}^K P^{(t)}(\mathbf{x}^{(y)}|\boldsymbol{\theta}) \log(P^{(t)}(\mathbf{x}^{(y)}|\boldsymbol{\theta})). \quad (6)$$

A comparison of PL/MP/NE is given in Sec. 4.2. In Fig. 4(a)-4(d), we calculate the most intuitive $S_{pl}(\mathbf{x})$ of inliers/outliers on benchmarks and visualize the normalized histograms of $S_{pl}(\mathbf{x})$, which are favorably separable for UOD. Besides, such results also verify the effectiveness of inlier priority.

4 Experiments

4.1 Experiment Setup

UOD Performance Evaluation on Image Benchmarks. We follow the standard procedure from previous image UOD literature [13, 16, 17] to construct an image set with outliers: Given a standard image benchmark, all images from a class with one common semantic concept (e.g. “horse”, “bag”) are retrieved as inliers, while outliers are randomly sampled from the rest of classes by an outlier ratio ρ . We vary ρ from 5% to 25% by a step of 5%. The assigned inlier/outlier labels are strictly unknown to UOD methods and only used for evaluation. Each class of a benchmark is used as inliers in turn and the performance on all classes is averaged as the overall UOD performance. The experiments are repeated for 5 times to report the average results. Five public benchmarks: MNIST [74], Fashion-MNIST (F-MNIST) [75], CIFAR10 [76], SVHN [77], CIFAR100 [76] are used for experiments³. Raw pixels are directly used as inputs with their intensity normalized into $[-1, 1]$. As for evaluation, we adopt the commonly-used Area under the Receiver Operating Characteristic curve (AUROC) and Area under the Precision-Recall curve (AUPR) as threshold-independent metrics [78].

Implementation Details and Compared Methods. For E^3 *Outlier*, we use an $n = 10$ layer wide ResNet (WRN) with a widen factor $k = 4$ as the backbone DNN architecture. $K = 111$ operations are used for surrogate supervision, and NE is used as the scoring strategy. Since surrogate supervision augments original data by K times, we train WRN for $\lceil \frac{250}{K} \rceil$ epochs. The batch size is 128. A learning rate 0.001 and a weight decay 0.0005 are adopted. The SGD optimizer with momentum 0.9 is used for MNIST and F-MNIST, while the Adam optimizer with $\beta = (0.9, 0.999)$ is used for CIFAR10, CIFAR100 and SVHN for better convergence. We compare E^3 *Outlier* with the baselines and existing state-of-the-art DNN based UOD methods (reviewed in Sec. 2) below: **1)** CAE [79]. It directly uses CAE’s reconstruction loss to perform UOD. **2)** CAE-IF. It feeds CAE’s learned representations into isolation forest (IF) [40] as explained in Sec. 3.1. **3)** Discriminative reconstruction based autoencoder (DRAE) [16]. **4)** Robust deep autoencoder (RDAE) [17]. **5)** Deep autoencoding gaussian mixture model (DAGMM) [18]. **6)** SSD-IF. It shares E^3 *Outlier*’s SSD part but feeds SSD’s learned representations into IF to perform UOD. For all AE based UOD methods above, we adopt the same CAE architecture from [58] with a 4-layer encoder and 4-layer decoder. We do not use more complex CAE (e.g. CAE using skip connection [80] or more layers) since they usually lower outliers’ reconstruction error as well and do not contribute to CAE’s UOD performance. The hyperparameters of the compared methods are set to recommended values (if provided) or the values that produce the best performance. More implementation details are given in Sec. 1 of the supplementary material. Our codes and results can be verified at <https://github.com/demonzyj56/E3outlier>.

4.2 UOD Performance Comparison and Discussion

UOD Performance Comparison. We report the numerical results on each benchmark under $\rho = 10\%$ and 20% in Table 1, and UOD performance by AUROC under ρ from 5% to 25% is shown in Fig. 5(a)-Fig. 5(e) (full results are given in Sec. 4 of supplementary material). AUPR-in and AUPR-out in Table 1 denote the AUPR calculated when inliers and outliers are used as positive class respectively. We draw the following observations from those results: Above all, E^3 *Outlier* overwhelmingly outperforms existing DNN based UOD methods by a large margin. As Table 1 shows, E^3 *Outlier* usually improves AUROC/AUPR by 5% to 30% when compared with state-of-the-art UOD methods. In particular, E^3 *Outlier* produces a significant performance leap

³As all images are viewed as unlabelled in UOD, we do not split train/test set. CIFAR100 uses 20 superclasses.

Table 1: AUROC/AUPR-in/AUPR-out (%) for UOD methods. The best performance is in bold.

Dataset	ρ	CAE	CAE-IF	DRAE	RDAE	DAGMM	SSD-IF	E^3 Outlier
MNIST	10%	68.0/92.0/32.9	85.5/97.8/49.0	66.9/93.0/30.5	71.8/93.1/35.8	64.0/92.9/26.6	93.8/99.2/68.7	94.1/99.3/67.5
	20%	64.0/82.7/40.7	81.5/93.6/57.2	67.2/86.6/42.5	67.0/84.2/43.2	65.9/86.4/41.3	90.5/97.3/71.0	91.3/97.6/72.3
F-MNIST	10%	70.3/94.3/29.3	82.3/97.2/40.3	67.1/93.9/25.5	75.3/95.8/31.7	64.0/92.7/30.3	90.6/98.5/68.6	93.3/99.0/75.9
	20%	64.4/85.3/36.8	77.8/92.2/49.0	65.7/86.9/36.6	70.9/89.2/41.4	66.0/86.7/43.5	87.6/95.6/71.4	91.2/97.1/78.9
CIFAR10	10%	55.9/91.0/14.4	54.1/90.2/13.7	56.0/90.7/14.7	55.4/90.7/14.0	56.1/91.3/15.6	64.0/93.5/18.3	83.5/97.5/43.4
	20%	54.7/81.6/25.5	53.8/80.7/25.3	55.6/81.7/26.8	54.2/81.0/25.7	54.7/81.8/26.3	60.2/85.0/28.3	79.3/93.1/52.7
SVHN	10%	51.2/90.3/10.6	55.0/91.4/11.9	51.0/90.3/10.5	52.1/90.6/10.8	50.0/90.0/19.3	73.4/95.9/22.0	86.0/98.0/36.7
	20%	50.7/80.2/20.7	54.0/82.0/22.4	50.6/80.4/20.5	51.8/80.9/21.1	50.0/79.9/29.6	69.2/89.5/33.7	81.0/93.4/47.0
CIFAR100	10%	55.2/91.0/14.5	54.5/90.7/13.8	55.6/90.9/15.0	55.8/90.9/15.0	54.9/91.1/14.2	55.6/91.5/13.0	79.2/96.8/33.3
	20%	54.4/81.7/25.6	53.5/80.9/25.1	55.5/81.8/27.0	54.9/81.5/26.5	53.8/81.5/24.7	54.3/82.1/23.4	77.0/92.4/46.5

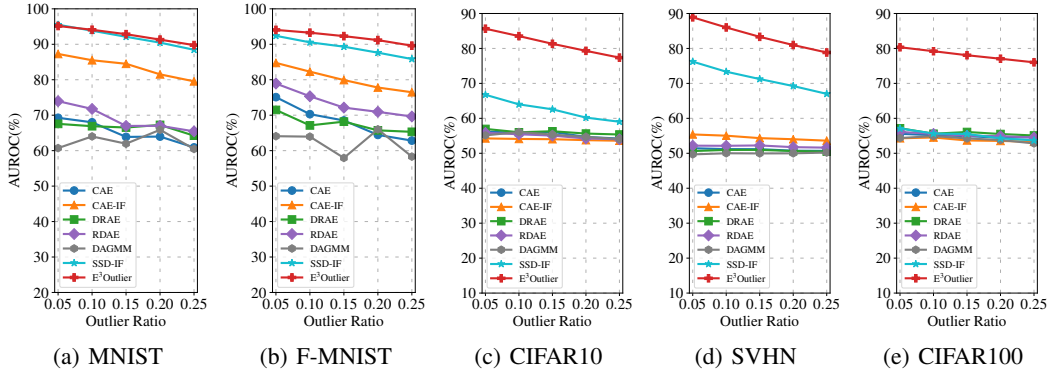


Figure 5: UOD performance (AUROC) comparison with varying ρ from 5% to 25%.

($\geq 20\%$ AUROC gain) on CIFAR10, SVHN and CIFAR100, which have constantly been difficult benchmarks for UOD. Next, end-to-end E^3 Outlier almost consistently outperforms its decoupled counterpart SSD-IF. Although SSD-IF performs closely to E^3 Outlier in simple cases, E^3 Outlier evidently prevails over SSD-IF on CIFAR10/SVHN/CIFAR100 by 11% to 24% AUROC gain. By contrast, the decoupled CAE-IF/RDAE get better UOD performance than their end-to-end counterparts CAE/DRAE/DAGMM on MNIST/F-MNIST, and all of them yield inferior performance on CIFAR10/SVHN/CIFAR100. Hence, observations above have justified E^3 Outlier as a highly effective and end-to-end UOD solution. In addition, we would like to make two remarks: **1)** We must point out that the data augmentation effect (surrogate supervision will augment the training data by K times) is not the reason why E^3 Outlier outperforms existing methods by a large margin. Experiments show that when we train CAE with the same training data with E^3 Outlier, the performance typically becomes worse than original CAE (e.g. 55.5%/63.9%/54.2%/50.0%/53.8% AUROC on MNIST/F-MNIST/CIFAR10/SVHN/CIFAR100 when $\rho = 10\%$). By contrast, E^3 Outlier can effectively exploit the high-level discriminative label information from data of pseudo classes, which is fundamentally different from generative models like AE/CAE. **2)** To fairly compare the quality of learned representation for CAE and SSD, CAE’s hidden layer by default shares SSD’s penultimate layer dimension, which is fixed to 256 by Wide-ResNet architecture. A different latent dimension may influence CAE’s performance, but it cannot enable CAE to perform comparably to E^3 Outlier, especially on difficult datasets like CIFAR10. We also test other values for CAE’s latent dimensions, and experimental results show that even for a carefully selected latent dimension (e.g. 64) that performs best on most benchmarks, it brings minimal gain to CAE’s performance on difficult datasets CIFAR10/CIFAR100 (e.g. 56.3%/56.1% AUROC when $\rho = 10\%$), and on simpler datasets (MNIST/F-MNIST/SVHN) CAE’s performance (71.9%/75.6%/53.4%, $\rho = 10\%$) is still far behind E^3 Outlier (94.1%/93.3%/86.0%) despite some limited improvement. More importantly, a prior choice of the optimal latent dimension or CAE architecture for UOD is difficult in itself.

Discussion. We discuss five factors that are related to our E^3 Outlier framework’s performance by experiments. Since the trends under different values of ρ are fairly similar, we visualize the results when using $\rho = 10\%$: **1)** Operation set for surrogate supervision (see Fig. 6(a)): We test the UOD

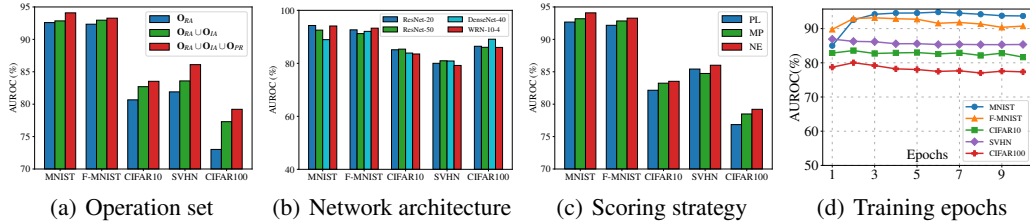


Figure 6: Different factors’ influence on $E^3Outlier$ ’s performance under $\rho = 10\%$.

performance with different combinations of operation subsets to be \mathcal{O} . The results suggest that \mathcal{O}_{RA} alone already works satisfactorily, but a union of \mathcal{O}_{RA} , \mathcal{O}_{IA} and \mathcal{O}_{PR} produces the best performance, which reflects the extensibility of operation sets. **2) Network architecture** (see Fig. 6(b)): In addition to WRN, we explore ResNet-20/ResNet-50 [19] and DenseNet-40 [81] for SSD with other settings fixed. The results show that those architectures basically achieve satisfactory UOD performance with minor differences, which verifies the applicability of different network architectures. In particular, we note that a more complex architecture (ResNet-50/DenseNet-40) improves the UOD performance on relatively complex datasets (CIFAR10, SVHN and CIFAR100), but its performance is inferior on simple datasets. **3) Scoring strategy** (see Fig. 6(c)): Among three scoring strategies (PL/MP/NE) proposed in Sec. 3.3, NE constantly yields the best performance by up to 2.3% AUC gain compared with PL/MP, while MP also outperforms the naive PL. Thus, we use the NE by default for $E^3Outlier$. **4) Training epochs** (see Fig. 6(d)): We measure the UOD performance when the SSD is trained by 1 to 10 epochs respectively. In general, the UOD performance is improved at the initial stage of training (less than 3 training epochs) and then stabilizes as the training epochs continue to increase. **5) Outlier ratio**: First, we note that sometimes the ratio of outliers can be very small (e.g. $\leq 1\%$), so we also test $E^3Outlier$ ’s performance in such case. The experiments show that $E^3Outlier$ still achieves satisfactory performance: For example, when $\rho = 0.5\%$, $E^3Outlier$ achieves 96.0%/93.6%/87.4%/91.0%/80.7% AUROC for MNIST/F-MNIST/CIFAR10/SVHN/CIFAR100 respectively, which is even better than the case with a higher outlier ratio. We also notice that the performance of $E^3Outlier$ tends to drop as the outlier ratio ρ increases. This is reasonable in the setting of UOD because the “outlierness” of outliers will decrease as their number increases, i.e. they are less likely to be viewed as “outliers” under the unsupervised setting as they gradually play a more important role in constituting the original unlabelled data.

5 Conclusion

In this paper, we propose a framework named $E^3Outlier$ to achieve effective and end-to-end UOD from raw image data. $E^3Outlier$ exploits surrogate supervision rather than traditional AE/CAE for representation learning in UOD, while a new property named inlier priority is demonstrated theoretically and empirically as the foundation of end-to-end UOD. By inlier priority and the negative entropy based score, $E^3Outlier$ achieves significant UOD performance leap when compared with state-of-the-art DNN based UOD methods. For future research, it is interesting to explore a quantitative measure of each operation’s effectiveness for surrogate supervision and develop effective late fusion strategies of different operations for scoring. As an open framework, different network architectures, surrogate supervision operations and scoring strategies can also be explored for $E^3Outlier$.

Acknowledgement

This work is supported by National Key R&D Program of China 2018YFB1003203 and National Natural Science Foundation of China (NSFC) under Grant No. 61773392, 61672528. This work is also supported by the German Research Foundation (DFG) award KL 2698/2-1 and by the German Federal Ministry of Education and Research (BMBF) awards 031L0023A, 01IS18051A, and 031B0770E. Xinwang Liu, En Zhu and Jianping Yin are corresponding authors of this paper.

References

- [1] Douglas M Hawkins. *Identification of outliers*, volume 11. Springer.
- [2] Varun Chandola, Arindam Banerjee, and Vipin Kumar. Anomaly detection: A survey. *ACM computing surveys (CSUR)*, 41(3):15, 2009.
- [3] Mohiuddin Ahmed, Abdun Naser Mahmood, and Md Rafiqul Islam. A survey of anomaly detection techniques in financial domain. *Future Generation Computer Systems*, 55:278–288, 2016.
- [4] Anna L Buczak and Erhan Guven. A survey of data mining and machine learning methods for cyber security intrusion detection. *IEEE Communications Surveys & Tutorials*, 18(2):1153–1176.
- [5] Alessandra De Paola, Salvatore Gaglio, Giuseppe Lo Re, Fabrizio Milazzo, and Marco Ortolani. Adaptive distributed outlier detection for wsns. *IEEE transactions on cybernetics*, 45(5):902–913, 2015.
- [6] Charu C Aggarwal. *Outlier Analysis*. Springer, 2016.
- [7] Varun Chandola and Vipin Kumar. Outlier detection : A survey. *Acm Computing Surveys*, 41(3), 2007.
- [8] Thomas Schlegl, Philipp Seeböck, Sebastian M Waldstein, Ursula Schmidt-Erfurth, and Georg Langs. Unsupervised anomaly detection with generative adversarial networks to guide marker discovery. In *International Conference on Information Processing in Medical Imaging*, pages 146–157. Springer, 2017.
- [9] B Ravi Kiran, Dilip Mathew Thomas, and Ranjith Parakkal. An overview of deep learning based methods for unsupervised and semi-supervised anomaly detection in videos. *Journal of Imaging*, 4(2):36, 2018.
- [10] Dan Hendrycks and Kevin Gimpel. A baseline for detecting misclassified and out-of-distribution examples in neural networks. *International Conference on Learning Representations*, 2017.
- [11] Shiyu Liang, Yixuan Li, and Rayadurgam Srikant. Enhancing the reliability of out-of-distribution image detection in neural networks. *International Conference on Learning Representations*, 2018.
- [12] Kimin Lee, Kibok Lee, Honglak Lee, and Jinwoo Shin. A simple unified framework for detecting out-of-distribution samples and adversarial attacks. *Neural Information Processing Systems*, pages 7167–7177, 2018.
- [13] Wei Liu, Gang Hua, and John R Smith. Unsupervised one-class learning for automatic outlier removal. In *Proceedings of the IEEE Conference on Computer Vision and Pattern Recognition*, pages 3826–3833, 2014.
- [14] Siqi Wang, Yijie Zeng, Qiang Liu, Chengzhang Zhu, En Zhu, and Jianping Yin. Detecting abnormality without knowing normality: A two-stage approach for unsupervised video abnormal event detection. In *2018 ACM Multimedia Conference on Multimedia Conference*, pages 636–644. ACM, 2018.
- [15] Yann LeCun, Yoshua Bengio, and Geoffrey Hinton. Deep learning. *nature*, 521(7553):436, 2015.
- [16] Yan Xia, Xudong Cao, Fang Wen, Gang Hua, and Jian Sun. Learning discriminative reconstructions for unsupervised outlier removal. In *Proceedings of the IEEE International Conference on Computer Vision (ICCV)*, pages 1511–1519, 2015.
- [17] Chong Zhou and Randy C Paffenroth. Anomaly detection with robust deep autoencoders. In *Proceedings of the 23rd ACM SIGKDD International Conference on Knowledge Discovery and Data Mining*, pages 665–674. ACM, 2017.

- [18] Bo Zong, Qi Song, Martin Renqiang Min, Wei Cheng, Cristian Lumezanu, Daeki Cho, and Haifeng Chen. Deep autoencoding gaussian mixture model for unsupervised anomaly detection. In *International Conference on Learning Representations (ICLR)*, 2018.
- [19] Kaiming He, Xiangyu Zhang, Shaoqing Ren, and Jian Sun. Deep residual learning for image recognition. In *Proceedings of the IEEE conference on computer vision and pattern recognition*, pages 770–778, 2016.
- [20] Raghavendra Chalapathy and Sanjay Chawla. Deep learning for anomaly detection: A survey. *arXiv preprint arXiv:1901.03407*, 2019.
- [21] Corinna Cortes and Vladimir Vapnik. Support-vector networks. *Machine learning*, 20(3):273–297, 1995.
- [22] Tin Kam Ho. The random subspace method for constructing decision forests. *IEEE Transactions on Pattern Analysis & Machine Intelligence*, (8):832–844, 1998.
- [23] Yue Zhao and Maciej K Hryniewicki. Xgbod: improving supervised outlier detection with unsupervised representation learning. In *2018 International Joint Conference on Neural Networks (IJCNN)*, pages 1–8. IEEE, 2018.
- [24] David Martinus Johannes Tax. One-class classification: Concept learning in the absence of counter-examples. 2002.
- [25] Markos Markou and Sameer Singh. Novelty detection: a review—part 1: statistical approaches. *Signal processing*, 83(12):2481–2497, 2003.
- [26] Bernhard Scholkopf, Ralf Herbrich, and Alexander J Smola. A generalized representer theorem. *European conference on computational learning theory*, pages 416–426, 2001.
- [27] David MJ Tax and Robert PW Duin. Support vector data description. *Machine learning*, 54(1):45–66, 2004.
- [28] Graham Williams, Rohan Baxter, Hongxing He, Simon Hawkins, and Lifang Gu. A comparative study of rnn for outlier detection in data mining. In *2002 IEEE International Conference on Data Mining, 2002. Proceedings.*, pages 709–712. IEEE, 2002.
- [29] Nathalie Japkowicz, Catherine Myers, and Mark Gluck. A novelty detection approach to classification. In *International Joint Conference on Artificial Intelligence*, pages 518–523, 1995.
- [30] Mei-ling Shyu, Shu-ching Chen, Kanoksri Sarinapakorn, and Liwu Chang. A novel anomaly detection scheme based on principal component classifier. In *in Proceedings of the IEEE Foundations and New Directions of Data Mining Workshop, in conjunction with the Third IEEE International Conference on Data Mining (ICDM'03)*. IEEE, 2003.
- [31] Heiko Hoffmann. Kernel pca for novelty detection. *Pattern recognition*, 40(3):863–874, 2007.
- [32] Frank E Grubbs. Procedures for detecting outlying observations in samples. *Technometrics*, 11(1):1–21, 1969.
- [33] Martin Ester, Hans-Peter Kriegel, Jörg Sander, Xiaowei Xu, et al. A density-based algorithm for discovering clusters in large spatial databases with noise. In *Kdd*, volume 96, pages 226–231, 1996.
- [34] Zengyou He, Xiaofei Xu, and Shengchun Deng. Discovering cluster-based local outliers. *Pattern Recognition Letters*, 24(9-10):1641–1650, 2003.
- [35] Markus M Breunig, Hans-Peter Kriegel, Raymond T Ng, and Jörg Sander. Lof: identifying density-based local outliers. In *ACM sigmod record*, volume 29, pages 93–104. ACM, 2000.
- [36] Emanuel Parzen. On estimation of a probability density function and mode. *The annals of mathematical statistics*, 33(3):1065–1076, 1962.
- [37] JooSeuk Kim and Clayton D Scott. Robust kernel density estimation. *Journal of Machine Learning Research*, 13(Sep):2529–2565, 2012.

- [38] Sridhar Ramaswamy, Rajeev Rastogi, and Kyuseok Shim. Efficient algorithms for mining outliers from large data sets. In *ACM Sigmod Record*, volume 29, pages 427–438. ACM, 2000.
- [39] Fabrizio Angiulli and Clara Pizzuti. Fast outlier detection in high dimensional spaces. In *European Conference on Principles of Data Mining and Knowledge Discovery*, pages 15–27. Springer, 2002.
- [40] Fei Tony Liu, Kai Ming Ting, and Zhi-Hua Zhou. Isolation forest. In *2008 Eighth IEEE International Conference on Data Mining*, pages 413–422. IEEE, 2008.
- [41] Fei Tony Liu, Kai Ming Ting, and Zhi-Hua Zhou. On detecting clustered anomalies using sciforest. In *Joint European Conference on Machine Learning and Knowledge Discovery in Databases*, pages 274–290. Springer, 2010.
- [42] Sunil Aryal, Kai Ming Ting, Jonathan R Wells, and Takashi Washio. Improving iforest with relative mass. In *Pacific-Asia Conference on Knowledge Discovery and Data Mining*, pages 510–521. Springer, 2014.
- [43] Chen Huang, Yining Li, Chen Change Loy, and Xiaoou Tang. Learning deep representation for imbalanced classification. In *Proceedings of the IEEE conference on computer vision and pattern recognition*, pages 5375–5384, 2016.
- [44] Salman H Khan, Munawar Hayat, Mohammed Bennamoun, Ferdous A Sohel, and Roberto Togneri. Cost-sensitive learning of deep feature representations from imbalanced data. *IEEE transactions on neural networks and learning systems*, 29(8):3573–3587, 2018.
- [45] Qi Dong, Shaogang Gong, and Xiatian Zhu. Imbalanced deep learning by minority class incremental rectification. *IEEE transactions on pattern analysis and machine intelligence*, 2018.
- [46] Chen Huang, Chen Change Loy, and Xiaoou Tang. Discriminative sparse neighbor approximation for imbalanced learning. *IEEE transactions on neural networks and learning systems*, 29(5):1503–1513, 2018.
- [47] Shuangfei Zhai, Yu Cheng, Weining Lu, and Zhongfei Zhang. Deep structured energy based models for anomaly detection. *international conference on machine learning*, pages 1100–1109, 2016.
- [48] Dan Xu, Yan Yan, Elisa Ricci, and Nicu Sebe. Detecting anomalous events in videos by learning deep representations of appearance and motion. *Computer Vision and Image Understanding*, 156:117–127, 2017.
- [49] Mahmudul Hasan, Jonghyun Choi, Jan Neumann, Amit K Roy-Chowdhury, and Larry S Davis. Learning temporal regularity in video sequences. In *Proceedings of the IEEE conference on computer vision and pattern recognition*, pages 733–742, 2016.
- [50] Yiru Zhao, Bing Deng, Chen Shen, Yao Liu, Hongtao Lu, and Xian-Sheng Hua. Spatio-temporal autoencoder for video anomaly detection. In *Proceedings of the 25th ACM international conference on Multimedia*, pages 1933–1941. ACM, 2017.
- [51] Lucas Deecke, Robert A Vandermeulen, Lukas Ruff, Stephan Mandt, and Marius Kloft. Anomaly detection with generative adversarial networks. In *European Conference on Principles of Data Mining and Knowledge Discovery*, pages 3–17, 2018.
- [52] Chu Wang, Yan-Ming Zhang, and Cheng-Lin Liu. Anomaly detection via minimum likelihood generative adversarial networks. In *2018 24th International Conference on Pattern Recognition (ICPR)*, pages 1121–1126. IEEE, 2018.
- [53] Thomas Schlegl, Philipp Seeböck, Sebastian M Waldstein, Georg Langs, and Ursula Schmidt-Erfurth. f-anogan: Fast unsupervised anomaly detection with generative adversarial networks. *Medical image analysis*, 54:30–44, 2019.
- [54] Lukas Ruff, Nico Görnitz, Lucas Deecke, Shoaib Ahmed Siddiqui, Robert Vandermeulen, Alexander Binder, Emmanuel Müller, and Marius Kloft. Deep one-class classification. In *International Conference on Machine Learning*, pages 4390–4399, 2018.

- [55] Raghavendra Chalapathy, Aditya Krishna Menon, and Sanjay Chawla. Anomaly detection using one-class neural networks. *arXiv preprint arXiv:1802.06360*, 2018.
- [56] Pramuditha Perera and Vishal M Patel. Learning deep features for one-class classification. *arXiv preprint arXiv:1801.05365*, 2018.
- [57] Patrick Schlachter, Yiwen Liao, and Bin Yang. Deep one-class classification using data splitting. *arXiv preprint arXiv:1902.01194*, 2019.
- [58] Izhak Golan and Ran El-Yaniv. Deep anomaly detection using geometric transformations. In *Advances in Neural Information Processing Systems*, pages 9758–9769, 2018.
- [59] Yezheng Liu, Zhe Li, Chong Zhou, Yuanchun Jiang, Jianshan Sun, Meng Wang, and Xiangnan He. Generative adversarial active learning for unsupervised outlier detection. *IEEE Transactions on Knowledge and Data Engineering*, 2019.
- [60] Nikos Komodakis and Spyros Gidaris. Unsupervised representation learning by predicting image rotations. In *International Conference on Learning Representations (ICLR)*, 2018.
- [61] Rodrigo Santa Cruz, Basura Fernando, Anoop Cherian, and Stephen Gould. Visual permutation learning. *IEEE Transactions on Pattern Analysis and Machine Intelligence*, 2018.
- [62] Xu Ji, Joao F Henriques, and Andrea Vedaldi. Invariant information clustering for unsupervised image classification and segmentation. *arXiv: Computer Vision and Pattern Recognition*, 2018.
- [63] Longlong Jing and Yingli Tian. Self-supervised visual feature learning with deep neural networks: A survey. *arXiv: Computer Vision and Pattern Recognition*, 2019.
- [64] Xi Peng, Jiashi Feng, Jiwen Lu, Wei-Yun Yau, and Zhang Yi. Cascade subspace clustering. In *Thirty-First AAAI Conference on Artificial Intelligence*, 2017.
- [65] Jianlong Chang, Lingfeng Wang, Gaofeng Meng, Shiming Xiang, and Chunhong Pan. Deep adaptive image clustering. In *Proceedings of the IEEE International Conference on Computer Vision*, pages 5879–5887, 2017.
- [66] Anders Boesen Lindbo Larsen, Søren Kaae Sønderby, Hugo Larochelle, and Ole Winther. Autoencoding beyond pixels using a learned similarity metric. In *International Conference on Machine Learning*, pages 1558–1566, 2016.
- [67] Alexey Dosovitskiy and Thomas Brox. Generating images with perceptual similarity metrics based on deep networks. In *Advances in neural information processing systems*, pages 658–666, 2016.
- [68] Sergey Zagoruyko and Nikos Komodakis. Wide residual networks. In *British Machine Vision Conference 2016*. British Machine Vision Association, 2016.
- [69] Andrew F Emmott, Shubhomoy Das, Thomas Dietterich, Alan Fern, and Weng-Keen Wong. Systematic construction of anomaly detection benchmarks from real data. In *Proceedings of the ACM SIGKDD workshop on outlier detection and description*, pages 16–21. ACM, 2013.
- [70] Haibo He and Eduardo A Garcia. Learning from imbalanced data. *IEEE Transactions on Knowledge & Data Engineering*, (9):1263–1284, 2008.
- [71] Justin M. Johnson and Taghi M. Khoshgoftaar. Survey on deep learning with class imbalance. *Journal of Big Data*, 6(1):27, 2019.
- [72] Léon Bottou. Online learning and stochastic approximations. *On-line learning in neural networks*, 17(9):142, 1998.
- [73] Thomas M Cover and Joy A Thomas. *Elements of information theory*. John Wiley & Sons, 2012.
- [74] Yann LeCun, Léon Bottou, Yoshua Bengio, Patrick Haffner, et al. Gradient-based learning applied to document recognition. *Proceedings of the IEEE*, 86(11):2278–2324, 1998.

- [75] Han Xiao, Kashif Rasul, and Roland Vollgraf. Fashion-mnist: a novel image dataset for benchmarking machine learning algorithms. *arXiv preprint arXiv:1708.07747*, 2017.
- [76] Alex Krizhevsky and Geoffrey Hinton. Learning multiple layers of features from tiny images. Technical report, Citeseer, 2009.
- [77] Yuval Netzer, Tao Wang, Adam Coates, Alessandro Bissacco, Bo Wu, and Andrew Y Ng. Reading digits in natural images with unsupervised feature learning. 2011.
- [78] Jesse Davis and Mark Goadrich. The relationship between precision-recall and roc curves. In *Proceedings of the 23rd international conference on Machine learning*, pages 233–240, 2006.
- [79] Jonathan Masci, Ueli Meier, Dan Cireşan, and Jürgen Schmidhuber. Stacked convolutional auto-encoders for hierarchical feature extraction. In *International Conference on Artificial Neural Networks*, pages 52–59. Springer, 2011.
- [80] Xiaojiao Mao, Chunhua Shen, and Yu-Bin Yang. Image restoration using very deep convolutional encoder-decoder networks with symmetric skip connections. In *Advances in neural information processing systems*, pages 2802–2810, 2016.
- [81] Gao Huang, Zhuang Liu, Laurens Van Der Maaten, and Kilian Q Weinberger. Densely connected convolutional networks. In *Proceedings of the IEEE conference on computer vision and pattern recognition*, pages 4700–4708, 2017.